Supporting Information to accompany

Redox, Spectroscopic and Magnetic Properties of C3-Symmetry Rare Earth Complexes Featuring Atypical Ortho-Dioxolene Binding

Stanley Bagio, Jonay González, Robert W. Gable, Christopher R. Hall, Colette Boskovic*, Marcus J. Giansiracusa*

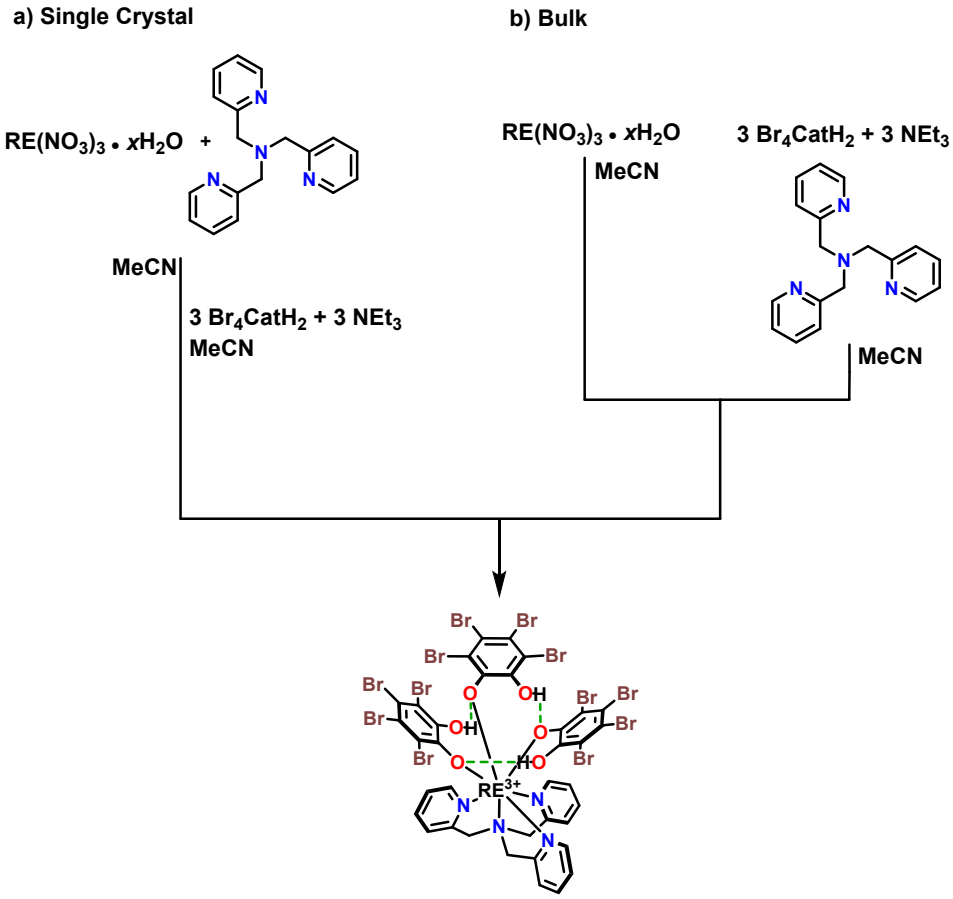

Scheme S1. Reaction scheme for [RE(Br$_4$catH)$_3$(tpa)] (**1-RE**) synthesis for (a) single crystal and (b) bulk samples.

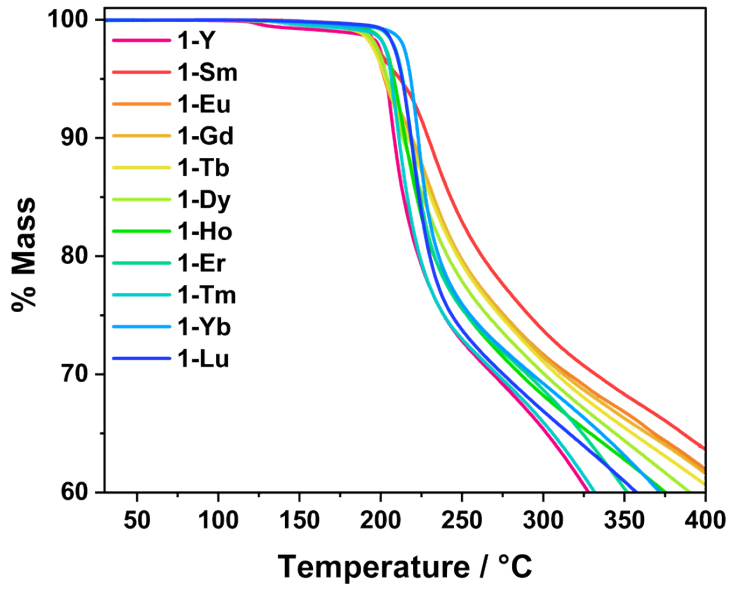

Figure S1. Thermogravimetric analysis (TGA) in the range 30-400°C under N_2 flow of **1-RE**·0.5MeCN.

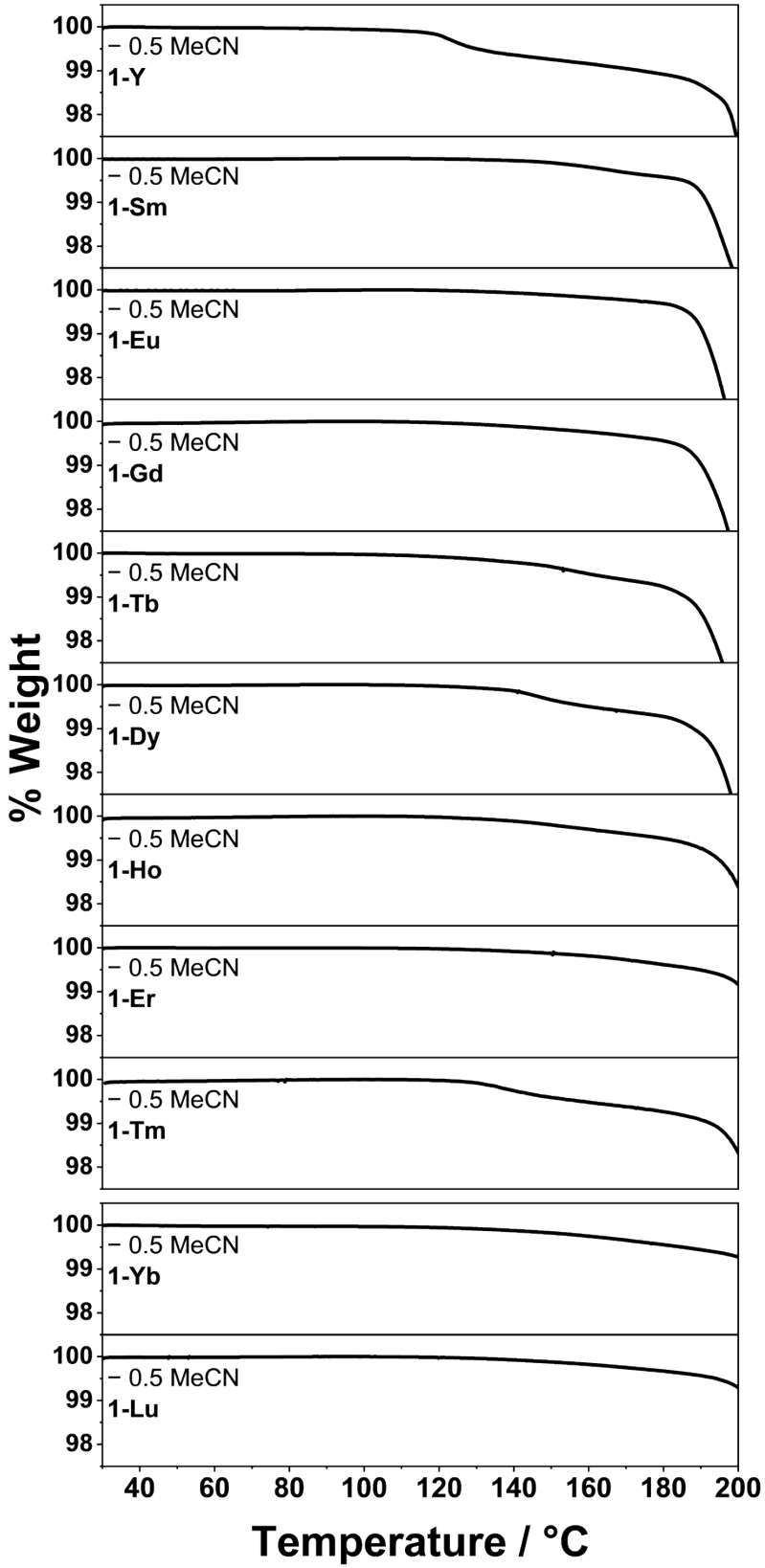

Figure S2. Thermogravimetric analysis (TGA) in the range 30-200°C under N_2 flow of **1-RE**·0.5MeCN.

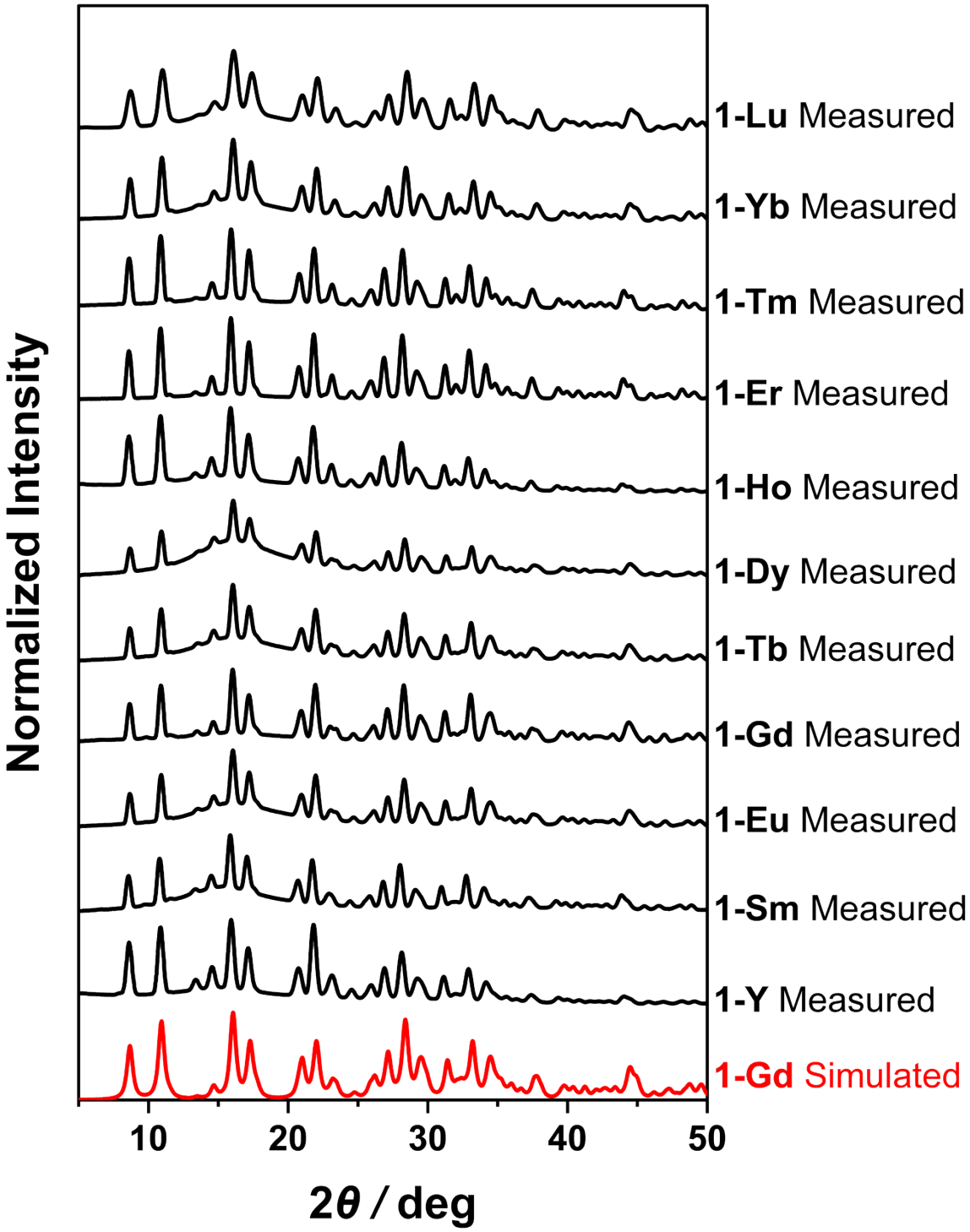

Figure S3. Experimental PXRD pattern for **1-RE**·0.5MeCN (100 K) vs simulated PXRD from **1-Gd** crystal structure (100 K).

Table S1. Crystallographic data and structure refinement parameters for compound **1-Y**, **1-Sm**, **1-Eu**, **1-Gd**, **1-Tb**, and **1-Dy**.

	1-Y	**1-Sm**	**1-Eu**	**1-Gd**	**1-Tb**	**1-Dy**
Empirical formula	$C_{36}H_{21}Br_{12}N_4O_6Y$	$C_{36}H_{21}Br_{12}N_4O_6Sm$	$C_{36}H_{21}Br_{12}N_4O_6Eu$	$C_{36}H_{21}Br_{12}N_4O_6Gd$	$C_{36}H_{21}Br_{12}N_4O_6Tb$	$C_{36}H_{21}Br_{12}N_4O_6Dy$
Formula weight	1653.28	1714.73	1716.34	1721.62	1723.3	1726.87
Temperature / K	100	100	100	100	100	100
Crystal system	trigonal	trigonal	trigonal	trigonal	trigonal	trigonal
Space group	*R*3*c*	*R*3*c*	*R*3*c*	*R*3*c*	*R*3*c*	*R*3*c*
a / Å	13.1340(2)	13.1753(1)	13.14725(1)	13.1452(1)	13.1128(1)	13.1174(1)
b / Å	13.1340(2)	13.1753(1)	13.14725(1)	13.1452(1)	13.1128(1)	13.1174(1)
c / Å	46.2582(7)	46.6188(4)	46.5427(7)	46.4914(7)	46.3988(7)	46.3156(6)
α / °	90	90	90	90	90	90
β / °	90	90	90	90	90	90
γ / °	120	120	120	120	120	120
Volume / Å^3	6910.6(2)	7008.30(12)	6967.05(15)	6957.25(15)	6909.21(15)	6901.66(14)
Z	6	6	6	6	6	6
ρ_{calc}g/cm^3	2.384	2.438	2.454	2.466	2.485	2.493
μ/mm^{-1}	14.384	21.863	22.164	21.764	20.153	21.305
F(000)	4632	4770	4776	4782	4788	4794
Crystal size / mm^3	0.09 × 0.08 × 0.06	0.07 × 0.04 × 0.03	0.08 × 0.07 × 0.06	0.04 × 0.03 × 0.02	0.06 × 0.04 × 0.01	0.09 × 0.07 × 0.07
Radiation	Cu Kα (λ = 1.54184)	Cu Kα (λ = 1.54184)	Cu Kα (λ = 1.54184)	Cu Kα (λ = 1.54184)	Cu Kα (λ = 1.54184)	Cu Kα (λ = 1.54184)
2θ range for data collection / °	8.67 to 160.836	8.67 to 160.837	8.67 to 160.838	8.67 to 160.839	8.67 to 160.840	8.67 to 160.841
Index ranges	-16 ≤ h ≤ 16, -16 ≤ k ≤ 16, -58 ≤ l ≤ 57	-16 ≤ h ≤ 16, -16 ≤ k ≤ 16, -59 ≤ l ≤ 48	-13 ≤ h ≤ 16, -16 ≤ k ≤ 16, -58 ≤ l ≤ 59	-16 ≤ h ≤ 15, -12 ≤ k ≤ 16, -59 ≤ l ≤ 58	-16 ≤ h ≤ 14, -16 ≤ k ≤ 16, -58 ≤ l ≤ 58	-16 ≤ h ≤ 16, -16 ≤ k ≤ 16, -58 ≤ l ≤ 51
Reflections collected	27677	29025	28401	28668	28311	27533
Independent reflections	3267 [R_{int} = 0.0642, R_{sigma} = 0.0334]	3222 [R_{int} = 0.0531, R_{sigma} = 0.0289]	3339 [R_{int} = 0.0416, R_{sigma} = 0.0224]	3342 [R_{int} = 0.0473, R_{sigma} = 0.0270]	3324 [R_{int} = 0.0588, R_{sigma} = 0.0306]	3084 [R_{int} = 0.0428, R_{sigma} = 0.0264]
Data/restraints/parameters	3267/1/179	3222/1/179	3339/1/179	3342/1/179	3324/1/179	3084/1/179
Goodness-of-fit on F^2	1.143	1.124	1.115	1.166	1.165	1.184
Final R indexes [I>=2σ (I)]	R_1 = 0.0361, wR_2 = 0.0941	R_1 = 0.0289, wR_2 = 0.0801	R_1 = 0.0239, wR_2 = 0.0658	R_1 = 0.0336, wR_2 = 0.0995	R_1 = 0.0365, wR_2 = 0.1034	R_1 = 0.0269, wR_2 = 0.0720
Final R indexes [all data]	R_1 = 0.0376, wR_2 = 0.0951	R_1 = 0.0293, wR_2 = 0.0804	R_1 = 0.0242, wR_2 = 0.0660	R_1 = 0.0339, wR_2 = 0.0998	R_1 = 0.0369, wR_2 = 0.1037	R_1 = 0.0272, wR_2 = 0.0722
Largest diff. peak/hole / eÅ^{-3}	0.98/-0.77	0.75/-1.23	0.58/-0.65	0.62/-1.01	0.63/-1.24	0.60/-0.63
Flack parameter	-0.02(3)	-0.015(2)	-0.0162(14)	-0.018(3)	-0.013(7)	-0.020(2)
CCDC Number	2405954	2405951	2405950	2405956	2405948	2405953

Table S2. Crystallographic data and structure refinement parameters for compound **1-Ho**, **1-Er**, **1-Tm**, **1-Yb**, and **1-Lu**.

	1-Ho	**1-Er**	**1-Tm**	**1-Yb**	**1-Lu**
Empirical formula	$C_{36}H_{21}Br_{12}N_4O_6Ho$	$C_{36}H_{21}Br_{12}N_4O_6Er$	$C_{36}H_{21}Br_{12}N_4O_6Tm$	$C_{36}H_{21}Br_{12}N_4O_6Yb$	$C_{36}H_{21}Br_{12}N_4O_6Lu$
Formula weight	1729.3	1731.63	1733.3	1737.41	1739.34
Temperature / K	100	100	100	100	100
Crystal system	trigonal	trigonal	trigonal	trigonal	trigonal
Space group	*R*3*c*	*R*3*c*	*R*3*c*	*R*3*c*	*R*3*c*
a / Å	13.1211(1)	13.1015(2)	13.0916(1)	13.1028(1)	13.0951(1)
b / Å	13.1211(1)	13.1015(2)	13.0916(1)	13.1028(1)	13.0951(1)
c / Å	46.2179(6)	46.1778(5)	46.0882(5)	45.9960(8)	45.9594(6)
α / °	90	90	90	90	90
β / °	90	90	90	90	90
γ / °	120	120	120	120	120
Volume / Å^3	6890.99(14)	6864.5(2)	6840.78(13)	6838.79(16)	6825.31(14)
Z	6	6	6	6	6
ρ_{calc}g/cm^3	2.5	2.513	2.524	2.531	2.539
μ/mm^{-1}	15.853	16.089	16.372	16.526	16.911
F(000)	4800	4806	4812	4818	4824
Crystal size / mm^3	0.06 × 0.04 × 0.01	0.09 × 0.07 × 0.07	0.08 × 0.07 × 0.06	0.06 × 0.04 × 0.01	0.09 × 0.07 × 0.07
Radiation	Cu Kα (λ = 1.54184)	Cu Kα (λ = 1.54184)	Cu Kα (λ = 1.54184)	Cu Kα (λ = 1.54184)	Cu Kα (λ = 1.54184)
2θ range for data collection / °	8.67 to 160.842	8.67 to 160.843	8.67 to 160.844	8.67 to 160.845	8.67 to 160.846
Index ranges	-15 ≤ h ≤ 16, -16 ≤ k ≤ 16, -58 ≤ l ≤ 58	-16 ≤ h ≤ 16, -16 ≤ k ≤ 16, -51 ≤ l ≤ 58	-16 ≤ h ≤ 16, -16 ≤ k ≤ 16, -58 ≤ l ≤ 56	-16 ≤ h ≤ 11, -16 ≤ k ≤ 16, -58 ≤ l ≤ 57	-15 ≤ h ≤ 16, -16 ≤ k ≤ 16, -56 ≤ l ≤ 58
Reflections collected	28061	26953	27886	27280	27160
Independent reflections	3308 [R_{int} = 0.0417, R_{sigma} = 0.0259]	3133 [R_{int} = 0.0831, R_{sigma} = 0.0535]	3227 [R_{int} = 0.0735, R_{sigma} = 0.0391]	3294 [R_{int} = 0.0473, R_{sigma} = 0.0250]	3234 [R_{int} = 0.0469, R_{sigma} = 0.0279]
Data/restraints/parameters	3308/1/179	3133/7/179	3227/1/179	3294/1/179	3234/1/179
Goodness-of-fit on F^2	1.164	1.125	1.151	1.193	1.176
Final R indexes [I>=2σ (I)]	R_1 = 0.0306, wR_2 = 0.0902	R_1 = 0.0435, wR_2 = 0.1137	R_1 = 0.0384, wR_2 = 0.1041	R_1 = 0.0264, wR_2 = 0.0764	R_1 = 0.0316, wR_2 = 0.0924
Final R indexes [all data]	R_1 = 0.0308, wR_2 = 0.0903	R_1 = 0.0474, wR_2 = 0.1169	R_1 = 0.0400, wR_2 = 0.1056	R_1 = 0.0265, wR_2 = 0.0765	R_1 = 0.0323, wR_2 = 0.0927
Largest diff. peak/hole / eÅ^{-3}	0.62/-1.01	1.49/-1.32	1.13/-1.56	0.70/-1.12	0.99/-1.94
Flack parameter	-0.046(10)	-0.02(3)	-0.02(2)	-0.021(9)	-0.01(2)
CCDC number	2405949	2405955	2405946	2405947	2405952

Table S3: Continuous SHAPE Measurements of **1-RE.**

	HP-7	HPY-7	PBPY-7	COC-7	CTPR-7	JPBPY-7	JETPY-7
1-Y	34.877	20.696	8.228	**0.660**	2.374	11.931	17.173
1-Sm	34.564	20.545	8.269	**0.855**	2.53	12.004	16.873
1-Eu	34.644	20.591	8.233	**0.791**	2.471	11.962	17.036
1-Gd	34.686	20.583	8.237	**0.766**	2.456	11.964	17.146
1-Tb	34.757	20.561	8.246	**0.717**	2.424	11.955	17.338
1-Dy	34.882	20.67	8.212	**0.658**	2.372	11.933	17.422
1-Ho	34.915	20.683	8.215	**0.659**	2.376	11.945	17.486
1-Er	34.969	20.694	8.212	**0.605**	2.334	11.923	17.544
1-Tm	34.995	20.704	8.203	**0.590**	2.323	11.921	17.639
1-Yb	35.121	20.779	8.192	**0.561**	2.301	11.924	17.855
1-Lu	35.183	20.782	8.204	**0.539**	2.292	11.939	17.985

Where HP-7 = Heptagon, HPY-7 = Hexagonal pyramid, PBPY-7 = Pentagonal bipyramid, COC-7 = Capped octahedron, CTPR-7 = Capped trigonal prism, JPBPY-7 = Johnson pentagonal bipyramid, JETPY-7 = Elongated triangular pyramid.

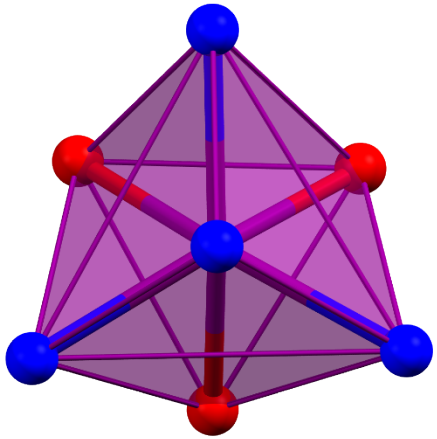

Figure S4. Coordination geometry of **1-RE** (capped octahedron) viewed along *c*-axis.

Table S4. CSoM values for 1-**Dy** Complex, all point Groups

Structure	All Atoms	Coordinated Atoms Only
Ci	81.869	190.616
Cs	16.234	0.072
C2	42.161	53.515
C2h	53.813	118.84
C2v	29.301	27.439
C3	0	0
C3h	39.624	82.261
C3v	8.117	0.036
C4	27.968	27.398
C4h	55.322	101.827
C4v	23.924	21.775
C5	25.415	22.33
C5h	53.104	96.014
C5v	22.965	19.882
C6	29.429	32.109
C7	23.737	21.225
C8	23.488	21.741
D2	59.648	101.609
D2d	52.839	87.087
D2h	54.581	101.863
D3	35.639	82.304
D3d	45.126	97.134
D3h	43.844	87.279
D4	53.688	100.118
D4d	48.731	89.385
D4h	53.269	97.557
D5	51.794	96.047
D5d	50.318	93.505
D5h	49.875	90.993
Oh	53.464	102.766
S4	57.705	101.582
S6	49.122	111.874
S8	55.343	100.094
S10	60.658	118.756

Table S5. CSoM values for all **1-RE** Complexes, for relevant point groups.

Structure	Cs	C3	C3v
Coordinated Atoms			
1-Y	0.096	0	0.048
1-Sm	0.127	0	0.063
1-Eu	0.101	0	0.051
1-Gd	0.111	0	0.055
1-Tb	0.058	0	0.029
1-Dy	0.072	0	0.036
1-Ho	0.070	0	0.035
1-Er	0.063	0	0.031
1-Tm	0.049	0	0.024
1-Yb	0.046	0	0.023
1-Lu	0.040	0	0.020
All atoms			
1-Y	16.207	0	8.104
1-Sm	16.266	0	8.133
1-Eu	16.283	0	8.142
1-Gd	16.263	0	8.132
1-Tb	16.245	0	8.123
1-Dy	16.234	0	8.117
1-Ho	16.224	0	8.112
1-Er	16.133	0	8.067
1-Tm	16.186	0	8.093
1-Yb	16.218	0	8.109
1-Lu	16.216	0	8.108

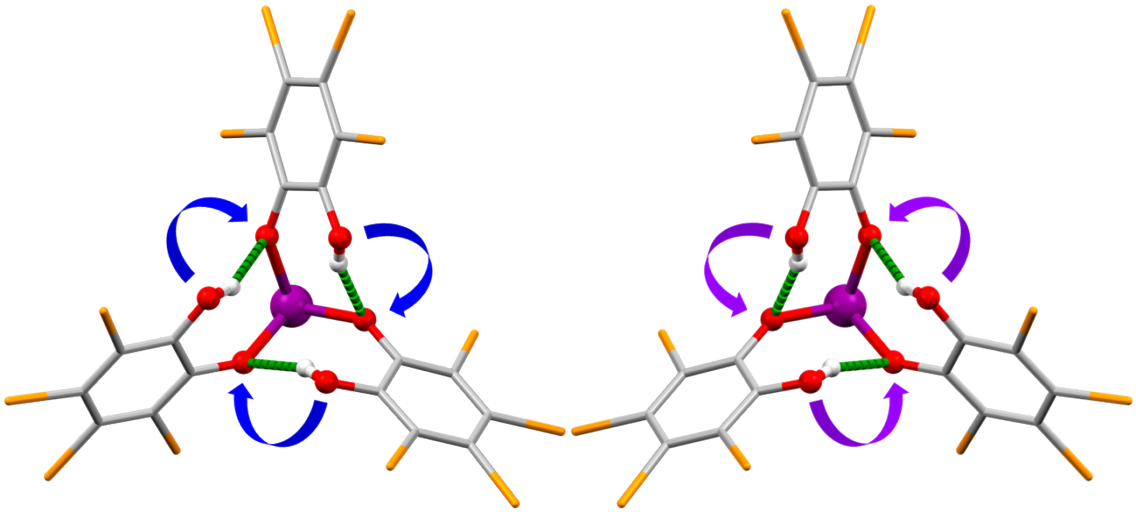

Figure S5. Enantiomers of **1-RE** with clockwise hydrogen-bonding (left, blue arrow) and anti-clockwise hydrogen-bonding (right, purple arrow). Tris(2-pyridylmethyl)amine and hydrogens not participating in H-bonding are removed for clarity. Colour code: C (grey), N (blue), O (red), Br (orange), H (white), RE (purple), H-bond (green).

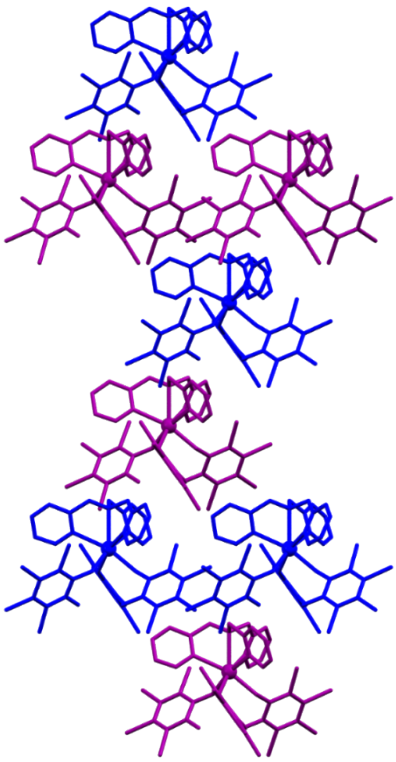

Figure S6: Crystal packing of **1-Gd** along *a*-axis. O1(H)···O2 H-bonding clockwise in blue and anticlockwise in purple.

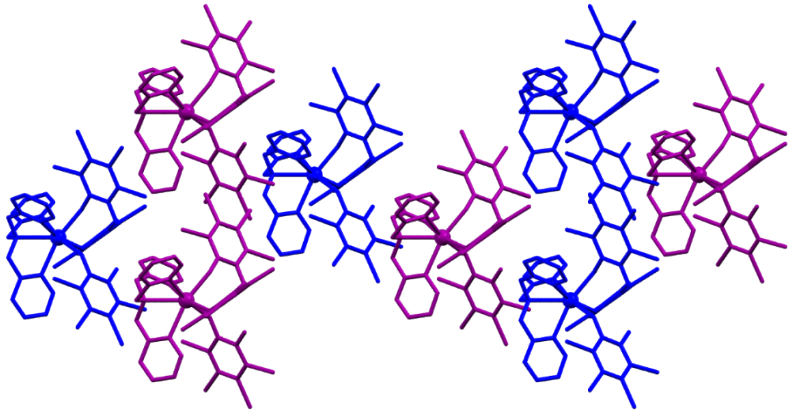

Figure S7. Crystal packing of **1-Gd** along *b*-axis. O1(H)···O2 H-bonding clockwise in blue and anticlockwise in purple.

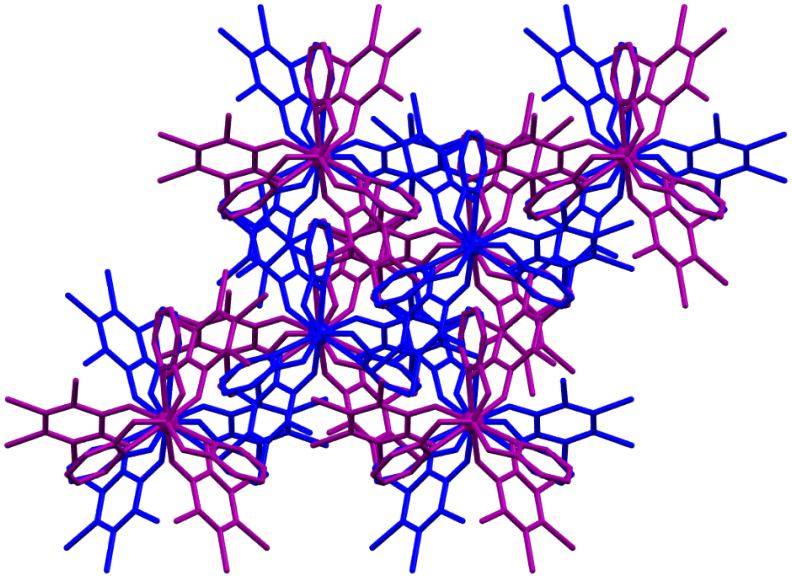

Figure S8. Crystal packing of **1-Gd** along *c*-axis. O1(H)···O2 H-bonding clockwise in blue and anticlockwise in purple.

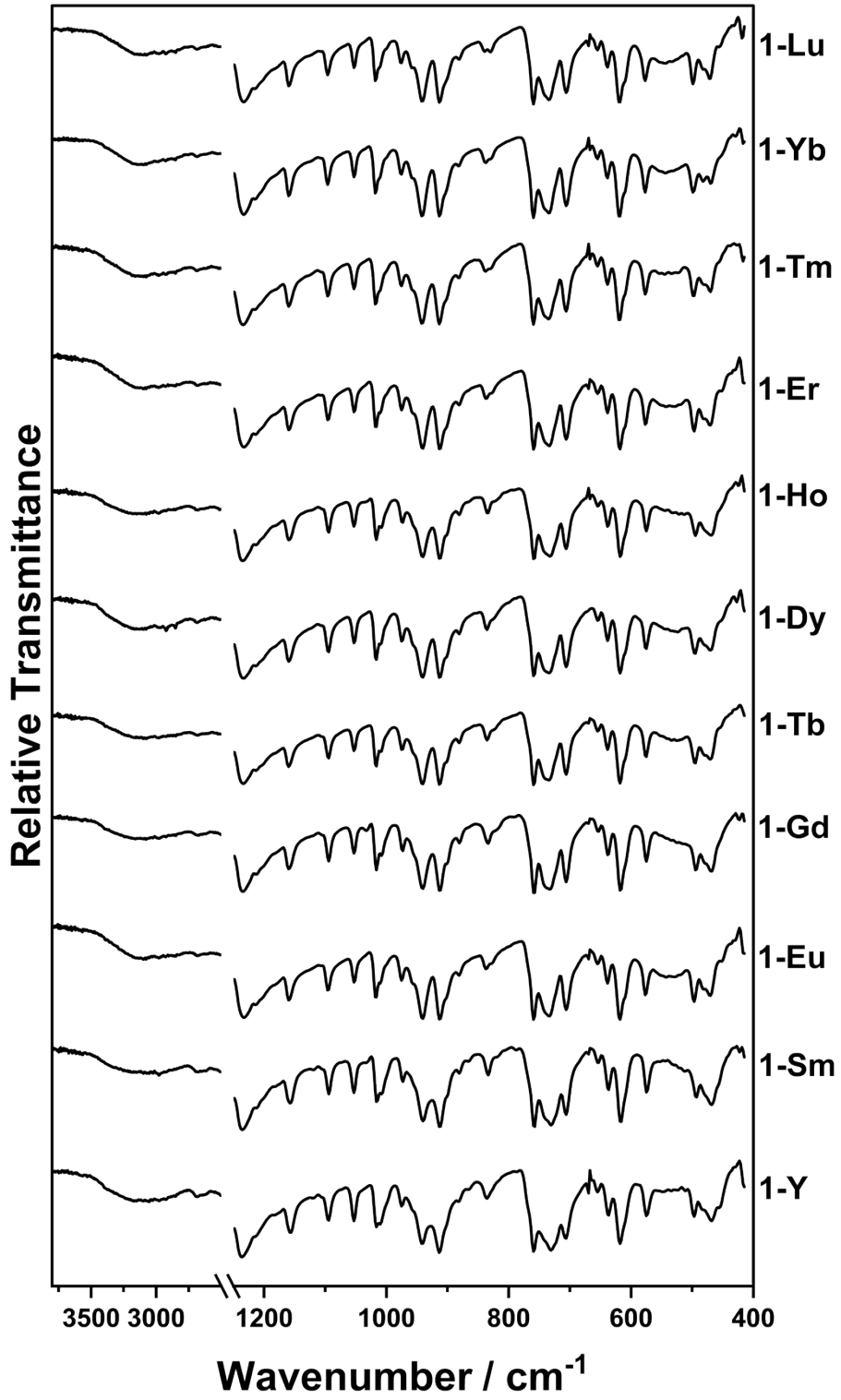

Figure S9. ATR-IR Spectra of **1-RE**·0.5MeCN.

Table S6. Selected IR (cm^{-1}) assignments of **1-RE**·0.5MeCN.

Moiety and Assignment[a]		1-Y	1-Sm	1-Eu	1-Gd	1-Tb	1-Dy	1-Ho	1-Er	1-Tm	1-Yb	1-Lu
cat	ν(O−H)	3100 (b)	3100 (b)	3100 (b)	3100 (b)	3100 (b)	3100 (b)	3100 (b)	3100 (b)	3100 (b)	3100 (b)	3100 (b)
tpa	ν(C=C)	1603 (m)	1601 (m)	1603 (m)	1603 (m)	1603 (m)	1603 (m)	1603 (m)	1603 (m)	1603 (m)	1603 (m)	1603 (m)
tpa	ν(C=N)	1572 (w)	1573 (w)	1571 (w)	1573 (w)	1573 (w)	1573 (w)	1573 (w)	1573 (w)	1573 (w)	1571 (w)	1573 (w)
cat	ν(C−O) + δ(C−H)	1443 (s)	1443 (s)	1433 (s)	1437 (s)	1435 (s)	1435 (s)	1435 (s)	1435 (s)	1435 (s)	1435 (s)	1435 (s)
cat	ν(C−O) + ν(C=C) + δ(C−H)	1316 (s)	1306 (s)	1311 (s)	1304 (s)	1306 (s)	1306 (s)	1308 (s)	1310 (s)	1314 (s)	1314 (s)	1306 (s)
cat	Skeletal diox	1256 (vw)	1258 (vw)	1261 (vw)	1258 (vw)	1258 (vw)	1258 (vw)	1258 (vw)	1258 (vw)	1258 (vw)	1258 (vw)	1258 (vw)
cat	ν(C−O) + ν(C−C)	1236 (s)	1236 (s)	1234 (s)	1236 (s)	1234 (s)	1234 (s)	1234 (s)	1234 (s)	1232 (s)	1232 (s)	1234 (s)

[a] Catecholate and tpa assignments based on literature DFT.[1]

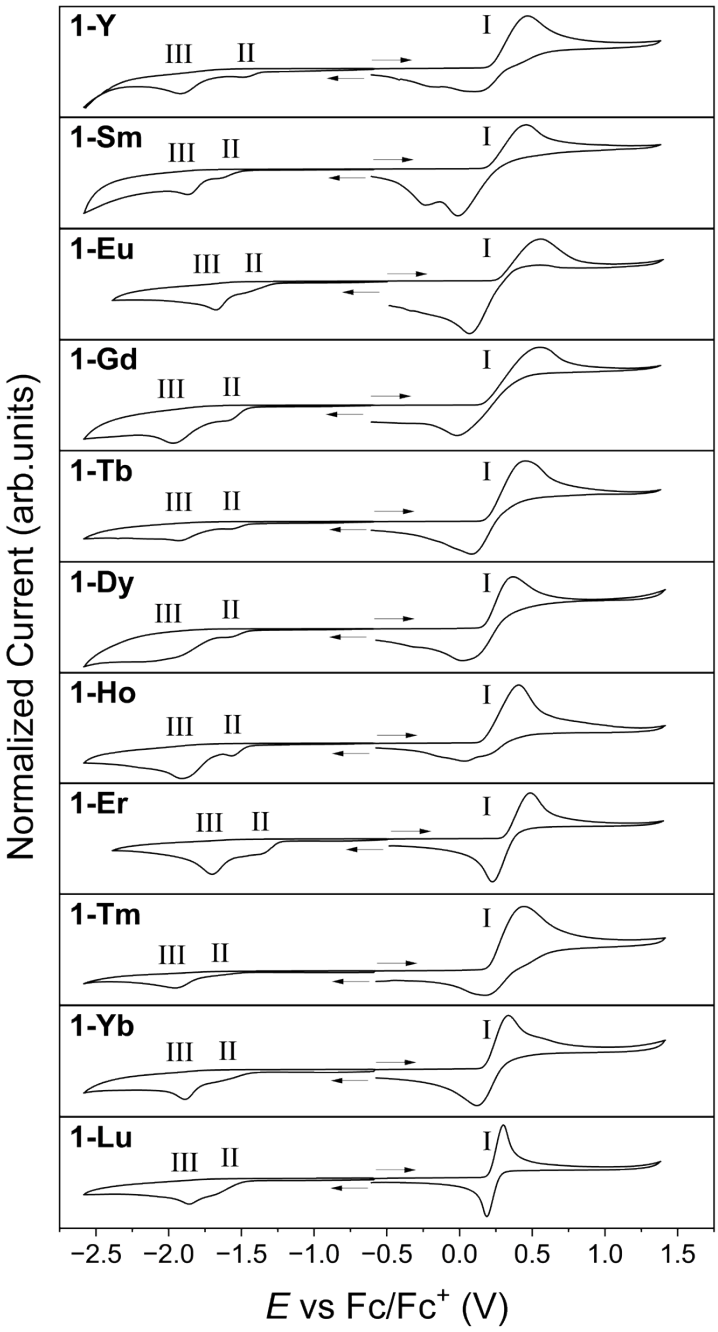

Figure S10. Cyclic voltammograms (between −2.75 and 1.75 V vs Fc/Fc^{+}) of a nafion-coated film of **1-RE** on a glassy carbon electrode in MeCN (0.25 M of TBAPF6) at a scan rate of 250 mVs^{-1}.Arrows indicate the starting potential and direction of scan.

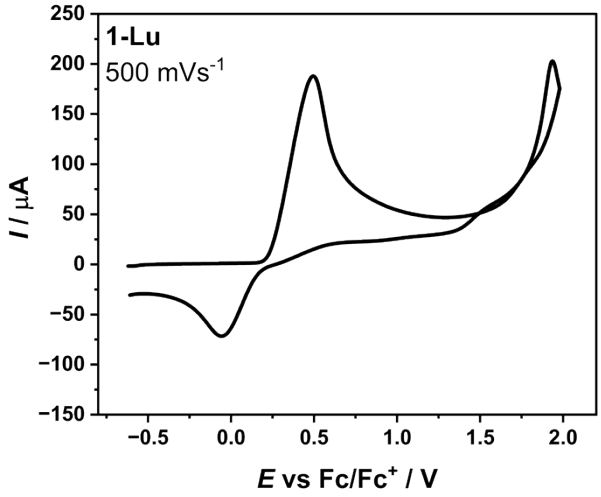

Figure S11. Cyclic voltammogram of **1-Lu** to solvent front at 500 mV s^{-1}.

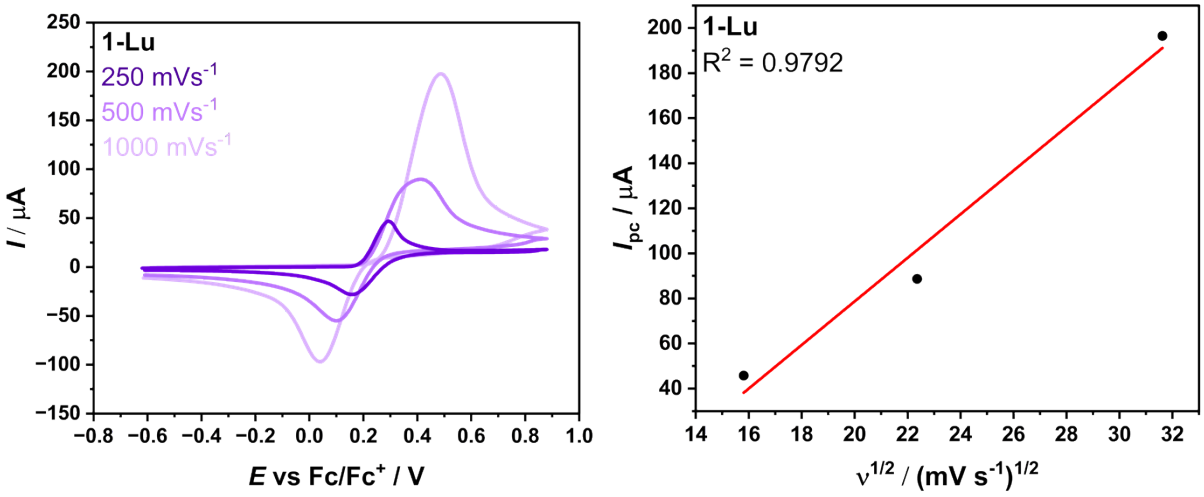

Figure S12. Left: Cyclic voltammograms for oxidation I of **1-Lu** at scan rates of 250, 500, and 1000 mVs^{-1} (top). Right: Plots of peak cathodic curent (I_{pc}) vs the square root of scan rate ($v^{1/2}$).

Table S7. Expected and measured room temperature $\chi_M T$ (cm^3 K mol^{-1}) M_{mol} ($N_A\mu_B$) values for **1-RE**·0.5MeCN.

1-RE	Theoretical $\chi_M T$ (cm^3 K mol^{-1})	Measured $\chi_M T$ (cm^3 K mol^{-1})	Theoretical M_{mol} ($N_A\mu_B$) at 2 K and 7 T	Measured M_{mol} ($N_A\mu_B$) at 2 K and 7 T
1-Sm	0.09	0.30	0.36	0.08
1-Eu	0	1.81	-	0.07
1-Gd	7.87	8.35	7.00	6.21
1-Tb	11.82	11.5	4.50	4.57
1-Dy	14.17	13.8	5.00	5.30
1-Ho	14.07	13.6	5.00	6.61
1-Er	11.48	11.2	4.50	4.90
1-Tm	7.15	7.07	3.50	2.18
1-Yb	2.57	2.24	2.00	1.70

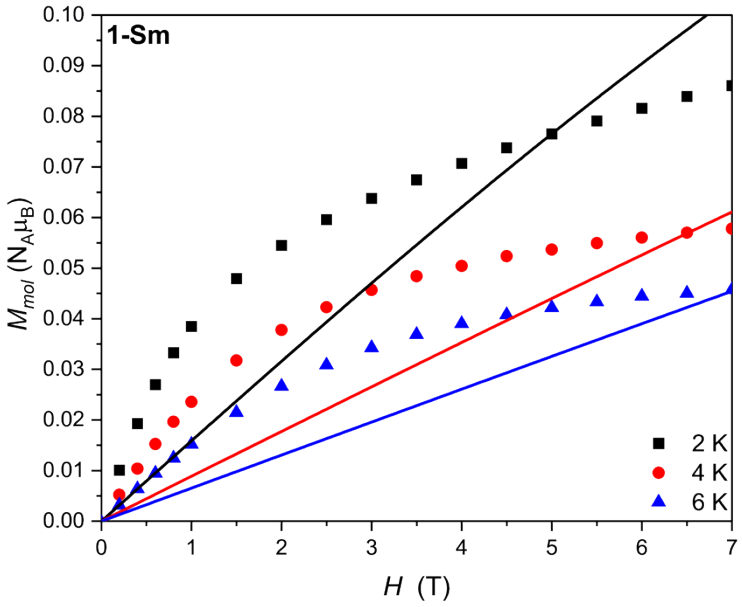

Figure S14. Measured magnetization data for **1-Sm**·0.5MeCN at 2 K (black squares), 4 K (red circles), 6 K (blue triangles) with calculated magnetization data at 2 K (solid black line), 4 K (solid red line), and 6 K (solid blue line).

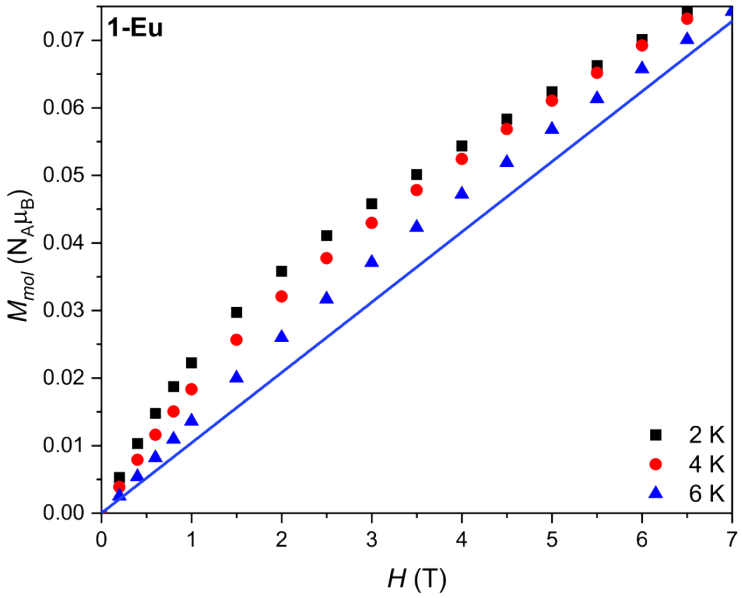

Figure S15. Measured magnetization data for **1-Eu**·0.5MeCN at 2 K (black squares), 4 K (red circles), 6 K (blue triangles) with calculated magnetization data at 2 K (solid black line), 4 K (solid red line), and 6 K (solid blue line).

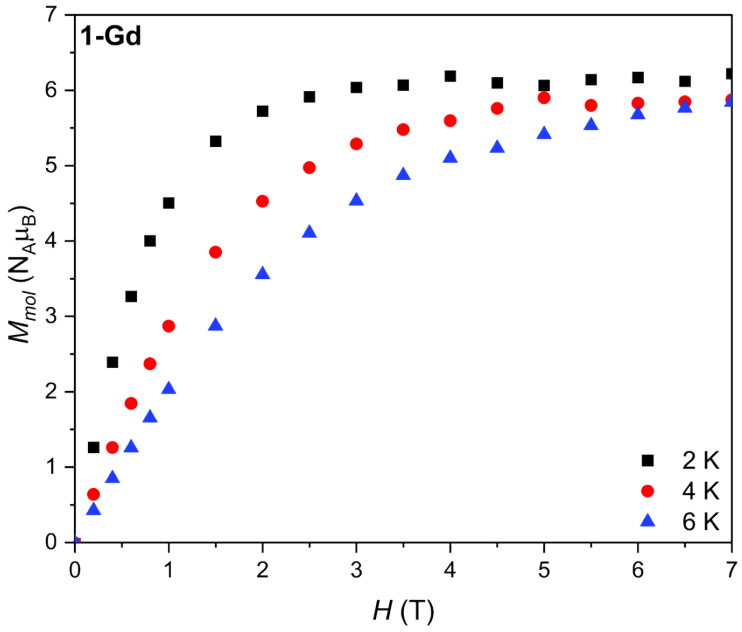

Figure S16. Measured magnetization data for **1-Gd**·0.5MeCN at 2 K (black squares), 4 K (red circles), 6 K (blue triangles).

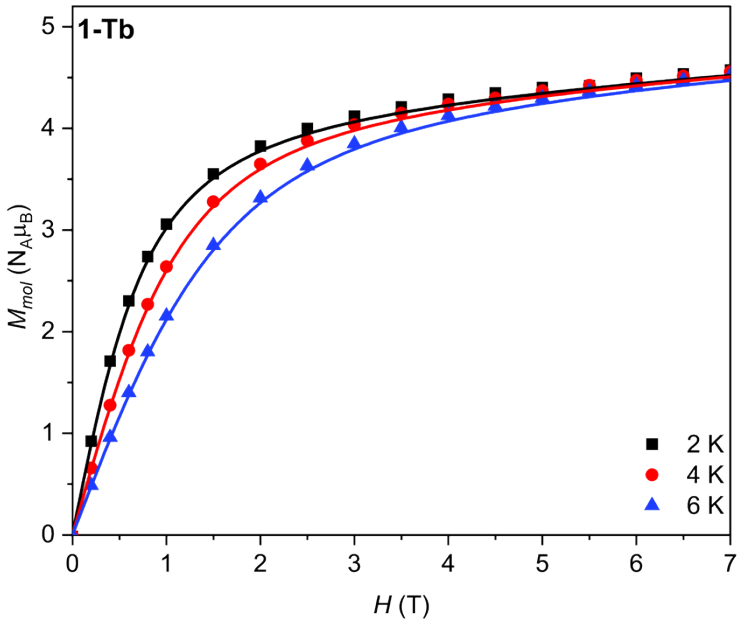

Figure S17. Measured magnetization data for **1-Tb**·0.5MeCN at 2 K (black squares), 4 K (red circles), 6 K (blue triangles) with calculated magnetization data at 2 K (solid black line), 4 K (solid red line), and 6 K (solid blue line).

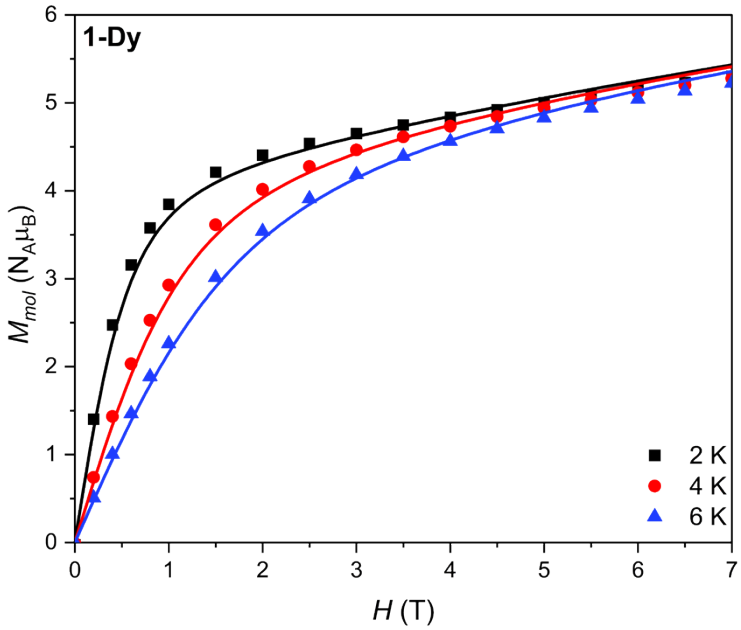

Figure S18. Measured magnetization data for **1-Dy**·0.5MeCN at 2 K (black squares), 4 K (red circles), 6 K (blue triangles) with calculated magnetization data at 2 K (solid black line), 4 K (solid red line), and 6 K (solid blue line).

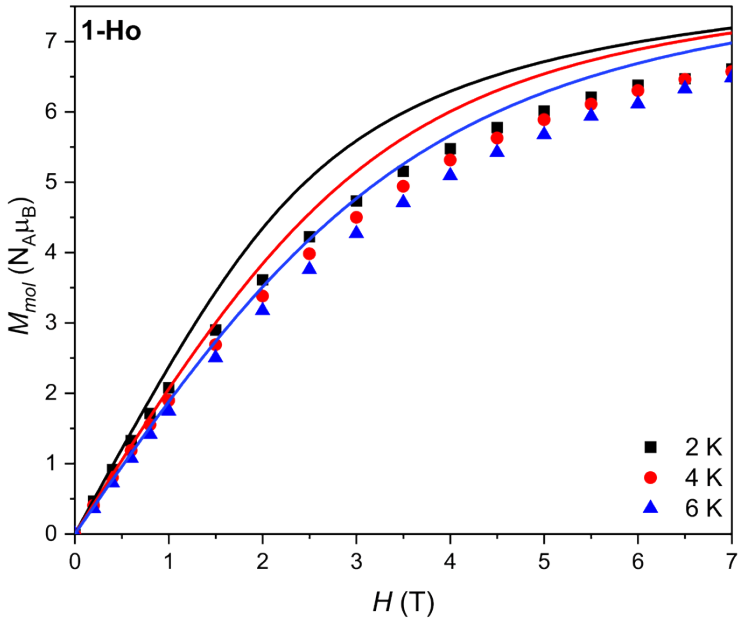

Figure S19. Measured magnetization data for **1-Ho**·0.5MeCN at 2 K (black squares), 4 K (red circles), 6 K (blue triangles) with calculated magnetization data at 2 K (solid black line), 4 K (solid red line), and 6 K (solid blue line).

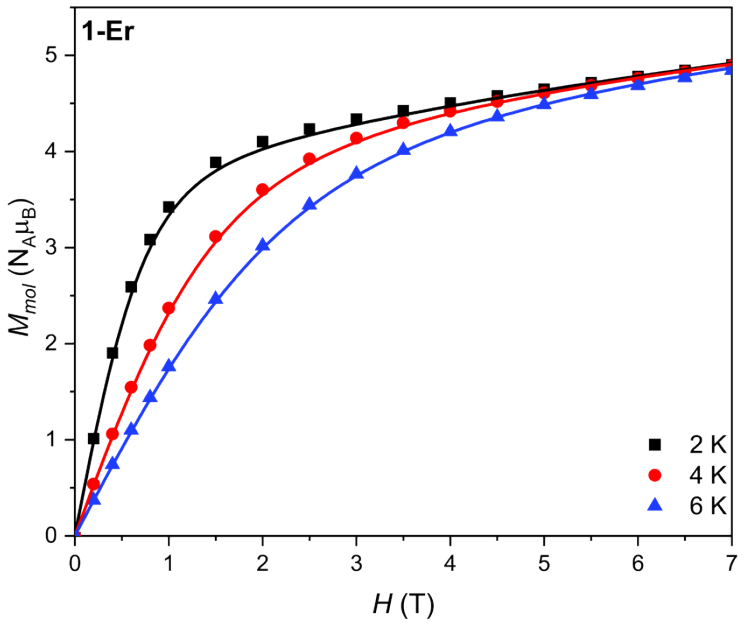

Figure S20. Measured magnetization data for **1-Er**·0.5MeCN at 2 K (black squares), 4 K (red circles), 6 K (blue triangles) with calculated magnetization data at 2 K (solid black line), 4 K (solid red line), and 6 K (solid blue line).

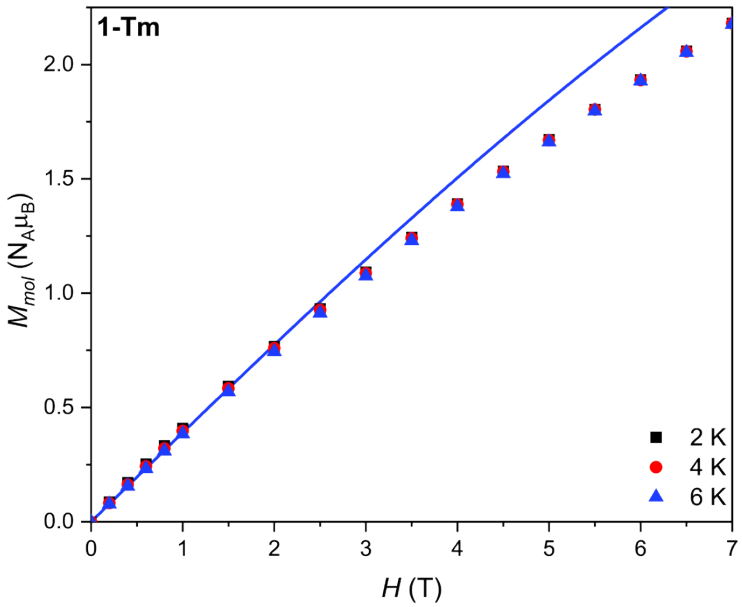

Figure S21. Measured magnetization data for **1-Tm**·0.5MeCN at 2 K (black squares), 4 K (red circles), 6 K (blue triangles) with calculated magnetization data at 2 K (solid black line), 4 K (solid red line), and 6 K (solid blue line).

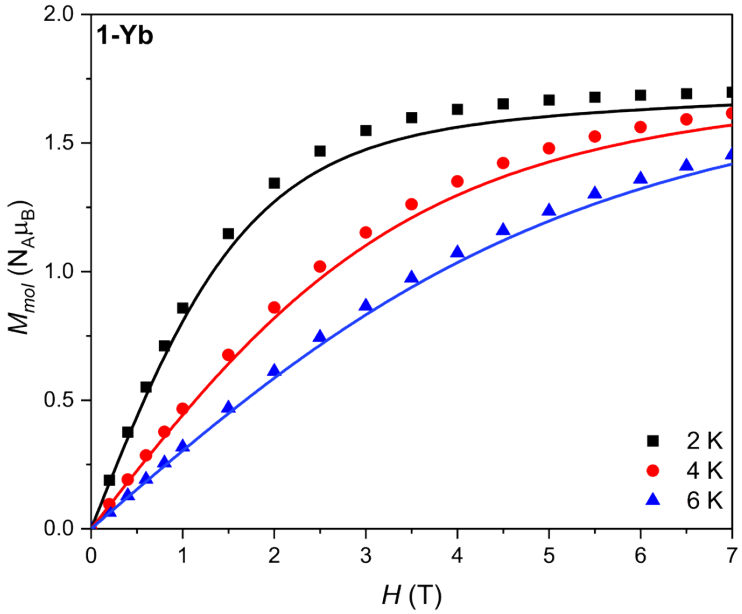

Figure S22. Measured magnetization data for **1-Yb**·0.5MeCN at 2 K (black squares), 4 K (red circles), 6 K (blue triangles) with calculated magnetization data at 2 K (solid black line), 4 K (solid red line), and 6 K (solid blue line).

Dynamic Magnetometry Studies

In phase (χ') and out-of-phase (χ'') were measured between 0.1-1000 Hz and both were fitted using the generalised Debye model, where χ_T is the isothermal susceptibility, χ_S adiabatic susceptibility, ω the angular frequency of the oscillating filed, τ the magnetic relaxation times, and α the distribution parameter.

$$\chi' = (\chi_T - \chi_S)\frac{(2\pi\omega\tau)^{1-\alpha}\cos(\frac{\alpha\pi}{2})}{1 + 2\sin\left(\frac{\alpha\pi}{2}\right)(2\pi\omega\tau)^{1-\alpha} + (2\pi\omega\tau)^{2-\alpha}} \quad \text{(Equation S1)}$$

$$\chi'' = (\chi_T - \chi_S)\frac{\cos(\frac{\pi\alpha}{2})(\omega\tau)^{1-\alpha}}{1 + 2\sin\left(\frac{\pi\alpha}{2}\right)(\omega\tau)^{1-\alpha} + (\omega\tau)^{2-2\alpha}} \quad \text{(Equation S2)}$$

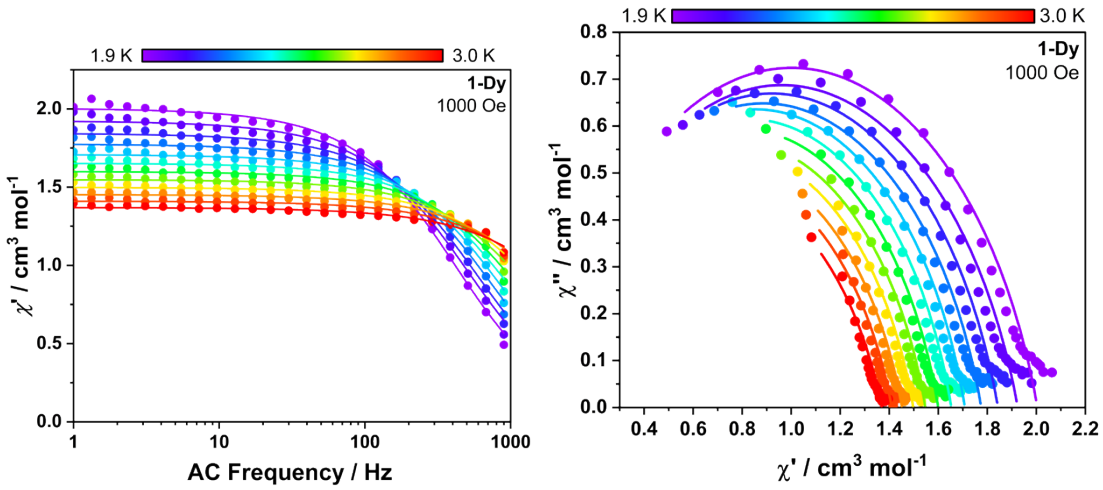

Figure S23. Left: Frequency dependence of the out-of-phase molar magnetic susceptibility of **1-Dy**·0.5MeCN in 1000 Oe. Right: Cole-Cole plots of **1-Dy**·0.5MeCN in 1000 Oe.

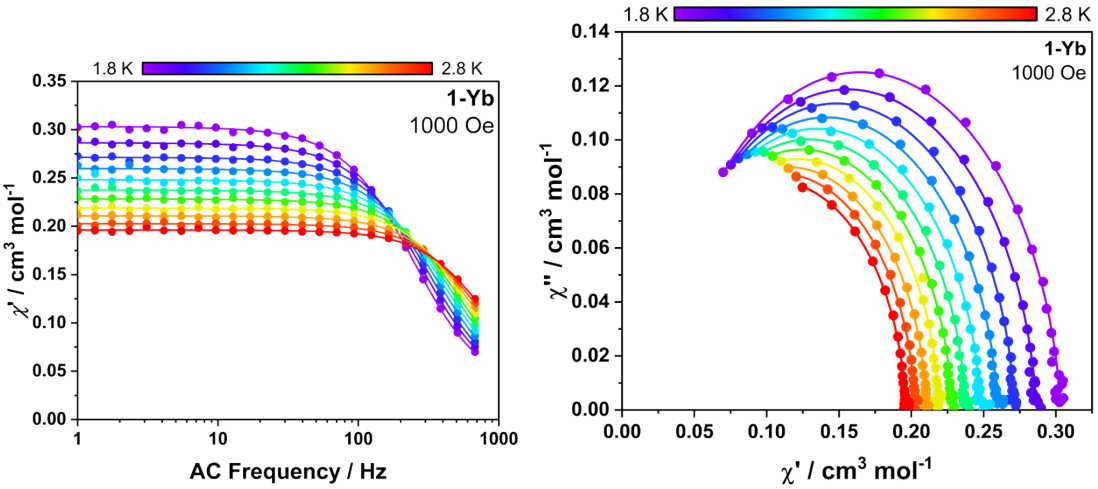

Figure S24. Left: Frequency dependence of the out-of-phase molar magnetic susceptibility of **1-Yb**·0.5MeCN in 1000 Oe. Right: Cole-Cole plots of **1-Yb**·0.5MeCN in 1000 Oe.

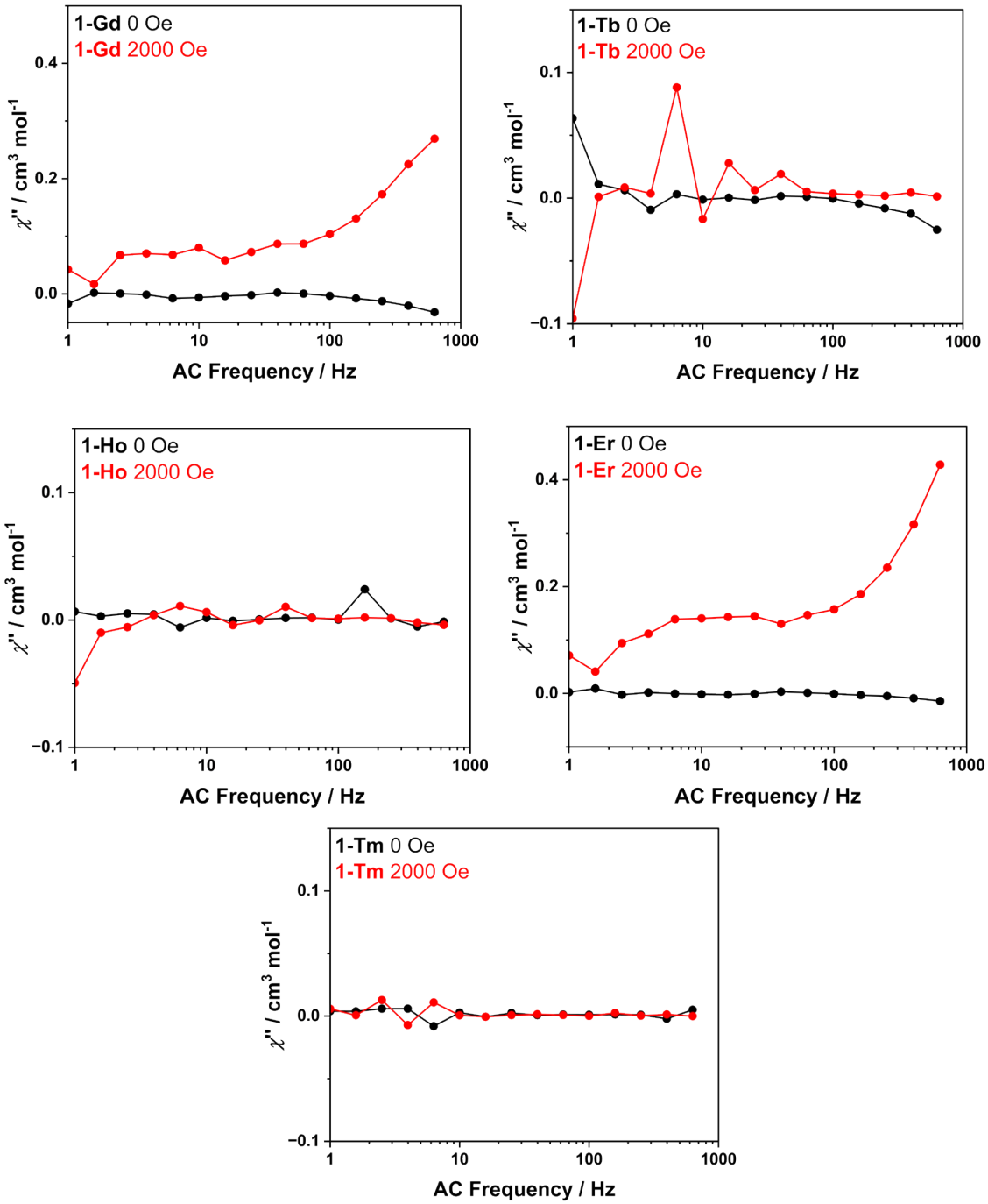

Figure S25. Frequency dependence of the out-of-phase molar magnetic susceptibility of **1-RE**·0.5MeCN (RE = Gd, Tb, Ho, Er, and Tm) at 0 and 2000 Oe at 2 K.

Table S8. Fitted parameters for **1-Dy** at 1000 Oe DC field by the generalised Debye Model.

T (K)	τ (s)	τ Std. Err.	a	χ_S (cm^3 mol^{-1})	χ_T (cm^3 mol^{-1})
1.9	3.84 E−04	1.99 E−05	0.20	0	2.00
2.0	3.13 E−04	2.10 E−05	0.21	0	1.92
2.1	2.62 E−04	2.62 E−05	0.20	0	1.84
2.2	2.18 E−04	1.85 E−05	0.20	0	1.78
2.3	1.80 E−04	1.66 E−05	0.19	0	1.71
2.4	1.50 E−04	1.64 E−05	0.19	0	1.65
2.5	1.24 E−04	1.67 E−05	0.19	0	1.60
2.6	1.01 E−04	1.62 E−05	0.19	0	1.55
2.7	8.22 E−05	1.53 E−05	0.20	0	1.50
2.8	6.60 E−05	1.64 E−05	0.20	0	1.50
2.9	5.63 E−05	1.79 E−05	0.21	0	1.41
3.0	4.53 E−05	1.71 E−05	0.23	0	1.37

Table S9. Fitted parameters for **1-Yb**·0.5MeCN at 1000 Oe DC field by the generalised Debye Model.

T (K)	τ (s)	τ Std. Err.	a	χ_S (cm^3 mol^{-1})	χ_T (cm^3 mol^{-1})
1.8	6.50E−4	5.53E−6	0.06	0.026	0.30
1.9	5.57E−4	5.10E−6	0.06	0.025	0.29
2.0	4.86E−4	4.39E−6	0.05	0.025	0.27
2.1	4.25E−4	5.41E−6	0.06	0.023	0.26
2.2	3.74E−4	6.26E−6	0.05	0.022	0.25
2.3	3.32E−4	4.61E−6	0.05	0.021	0.24
2.4	2.97E−4	4.41E−6	0.05	0.021	0.23
2.5	2.70E−4	7.17E−6	0.03	0.024	0.22
2.6	2.37E−4	2.94E−6	0.04	0.020	0.21
2.7	2.10E−4	5.37E−6	0.04	0.018	0.20
2.8	1.88E−4	5.33E−6	0.04	0.016	0.20

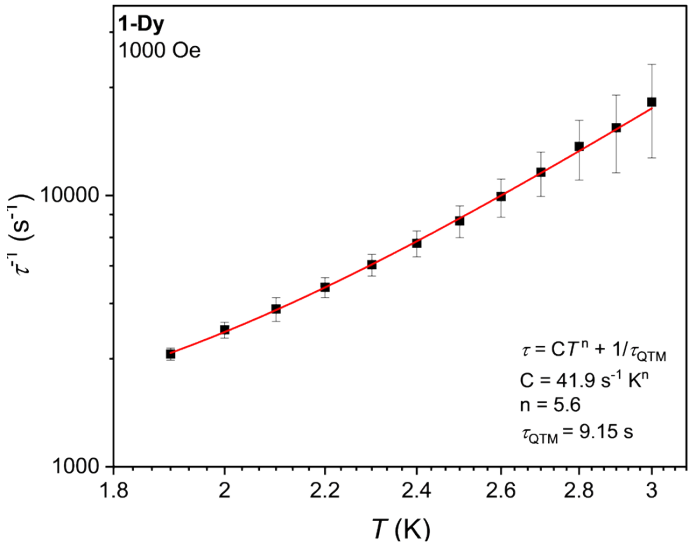

Figure S26. Relaxation rates of **1-Dy**·0.5MeCN as determined by AC susceptibility measurement (data points) and QTM and Raman relaxation fit (red line).

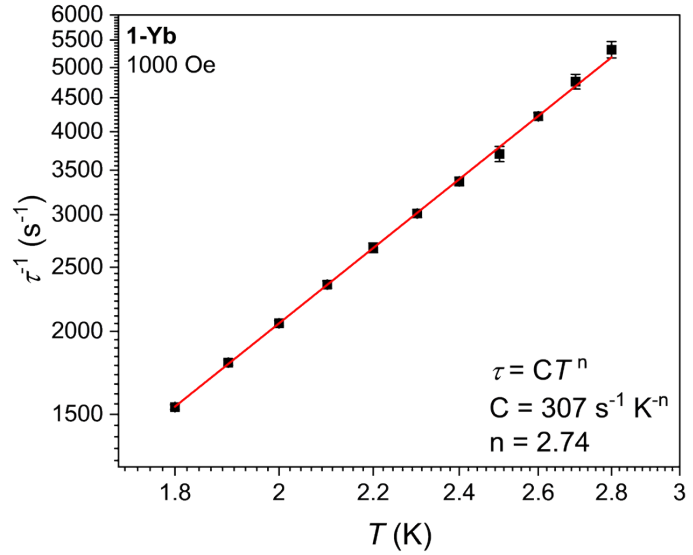

Figure S27. Relaxation rates of **1-Yb**·0.5MeCN as determined by AC susceptibility measurement (data points) and Raman relaxation fit (red line) represented as log-log plot.

Table S10. Energies (cm^{-1}), percentage composition of the CASSCF/RASSI wavefunctions and the principal *g* values of **1-Sm.**

	$\|m_J>$					
Energy (cm^{-1})	**5/2**	**3/2**	**1/2**	**−1/2**	**−3/2**	**−5/2**
0.00	0.9	0.0	49.1	49.0	0.0	0.9
115.3	0.0	97.6	0.0	0.0	2.4	0.0
249.9	0.0	0.0	1.9	0.0	0.0	98.1

	Principal *g* values		
Energy (cm^{-1})	g_x	g_y	g_z
0.00	0.48	0.48	0.19
115.3	0.48	0.48	0.19
249.9	0.00	0.00	1.41

Table S11. Energies (cm^{-1}), percentage composition of the CASSCF/RASSI wavefunctions and the principal *g* values of **1-Tb.**

	$\|m_J>$												
Energy (cm^{-1})	**6**	**5**	**4**	**3**	**2**	**1**	**0**	**−1**	**−2**	**−3**	**−4**	**−5**	**−6**
0.00	40.8	0.0	0.0	7.3	0.0	0.0	3.7	0.0	0.0	7.3	0.0	0.0	40.8
4.28	44.2	0.0	0.0	5.7	0.0	0.0	0.0	0.0	0.0	5.7	0.0	0.0	44.3
101.5	0.0	29.6	1.2	0.0	16.4	2.8	0.0	2.8	16.4	0.0	1.2	29.6	0.0
101.5	0.0	29.6	1.2	0.0	16.4	2.8	0.0	2.8	16.4	0.0	1.2	29.6	0.0
151.3	0.0	3.1	26.3	0.0	0.8	19.8	0.0	19.8	0.8	0.0	26.3	3.1	0.0
151.3	0.0	3.1	26.3	0.0	0.8	19.8	0.0	19.8	0.8	0.0	26.3	3.1	00.
194.5	7.7	0.0	0.0	15.8	0.0	0.0	53.0	0.0	0.0	15.8	0.0	0.0	7.7
319.3	5.7	0.0	0.0	44.3	0.0	0.0	0.04	0.0	0.0	44.3	0.0	0.0	5.7
395.8	0.0	14.3	6.9	0.0	22.6	6.3	0.0	6.3	22.6	0.0	6.9	14.3	0.0
395.8	0.0	14.3	6.9	0.0	22.6	6.3	0.0	6.3	22.6	0.0	6.9	14.3	0.0
452.5	0.0	3.1	15.6	0.0	10.2	21.1	0.0	21.1	10.2	0.0	15.6	3.1	0.0
452.5	0.0	3.1	15.6	0.0	10.2	21.1	0.0	21.1	10.2	0.0	15.6	3.1	0.0
463.5	1.4	0.0	0.0	27.0	0.0	0.0	43.2	0.0	0.0	27.0	0.0	0.0	1.4

	Principal *g* values		
Energy (cm^{-1})	g_x	g_y	g_z
0.00	0.0	0.0	16.51
4.28	0.0	0.0	16.51
101.5	0.0	0.0	10.59
101.5	0.0	0.0	10.59
151.3	0.0	0.0	6.85
151.3	0.0	0.0	6.85
194.5	0.0	0.0	0.00
319.3	0.0	0.0	0.00
395.8	0.0	0.0	3.87
395.8	0.0	0.0	3.87
452.5	0.0	0.0	1.73
452.5	0.0	0.0	1.73
463.5	0.0	0.0	0.00

Table S12. Energies (cm^{-1}), percentage composition of the CASSCF/RASSI wavefunctions and the principal *g* values of **1-Dy.**

	$\|m_J\rangle$															
Energy (cm^{-1})	**+15/2**	**+13/2**	**+11/2**	**+9/2**	**+7/2**	**+5/2**	**+3/2**	**+1/2**	**−1/2**	**−3/2**	**−5/2**	**−7/2**	**−9/2**	**−11/2**	**−13/2**	**−15/2**
0.00	0.0	13.0	0.9	0.0	3.2	1.3	0.0	0.3	1.3	0.0	0.3	15.5	0.0	0.2	64.1	0.0
56.4	0.0	1.6	32.8	0.0	0.0	11.4	0.0	0.1	0.1	0.0	13.6	0.0	0.0	39.0	1.4	0.0
89.4	17.7	0.0	0.0	33.8	0.0	0.0	19.0	0.0	0.0	4.3	0.0	0.0	16.3	0.0	0.0	8.9
194.8	0.0	8.2	0.8	0.0	13.3	0.8	0.0	53.5	11.3	0.0	3.6	2.8	0.0	3.9	1.7	0.0
231.3	0.0	0.0	0.0	0.0	0.0	0.0	1.9	0.0	0.0	28.2	0.0	0.0	4.6	0.0	0.0	65.3
448.4	0.0	3.8	0.2	0.0	24.4	0.6	0.0	8.1	0.1	0.0	47.1	0.3	0.0	15.4	0.0	0.0
467.6	0.1	0.0	0.0	0.7	0.0	0.0	1.5	0.0	0.0	45.1	0.0	0.0	44.6	0.0	0.0	8.0
571.9	0.0	5.9	0.0	0.0	40.3	0.1	0.0	24.1	0.1	0.0	21.3	0.2	0.0	6.8	0.0	0.0

	Principal *g* values		
Energy (cm^{-1})	g_x	g_y	g_z
0.00	14.81	2.51	2.51
56.4	11.55	2.11	2.11
89.4	12.01	0.00	0.00
194.8	9.50	3.10	9.50
231.3	14.60	0.00	0.00
448.4	8.64	2.38	8.64
467.6	8.66	0.00	0.01
571.9	9.09	2.70	9.08

Table S13. Energies (cm^{-1}), percentage composition of the CASSCF/RASSI wavefunctions and the principal *g* values of **1-Ho.**

	$\|m_J>$																
Energy (cm^{-1})	**8**	**7**	**6**	**5**	**4**	**3**	**2**	**1**	**0**	**−1**	**−2**	**−3**	**−4**	**−5**	**−6**	**−7**	**−8**
0.00	9.5	1.1	0.0	14.1	16.0	0.0	9.1	0.2	0.0	0.2	9..1	0.0	16.0	14.1	0.0	1.1	9.5
0.00	9.5	1.1	0.0	14.4	16.0	0.0	9.1	0.2	0.0	0.2	9.1	0.0	16.0	14.1	0.0	1.1	9.5
12.7	0.0	0.0	7.7	0.0	0.0	41.9	0.0	0.0	0.7	0.0	0.0	41.9	0.0	0.0	7.7	0.0	0.0
17.9	9.2	2.3	0.0	9.8	23.6	0.0	0.1	4.9	0.0	4.9	0.1	0.0	23.6	9.8	0.0	2.3	9.2
17.9	9.2	2.3	0.0	9.9	23.6	0.0	0.1	4.9	0.0	4.9	0.1	0.0	23.6	9.9	0.0	2.3	9.2
80.0	0.0	0.0	18.0	0.0	0.0	25.4	0.0	0.0	13.2	0.0	0.0	25.3	0.0	0.0	18.0	0.0	0.0
104.3	30.8	0.1	0.0	11.5	0.3	0.0	5.2	2.1	0.0	2.1	5.2	0.0	0.3	11.5	0.0	0.1	30.8
104.3	30.8	0.1	0.0	11.5	0.3	0.0	5.2	2.1	0.0	2.1	5.2	0.0	0.3	11.5	0.0	0.1	30.8
259.4	0.0	0.0	42.3	0.0	0.0	7.7	0.0	0.0	0.0	0.0	0.0	7.7	0.0	0.0	41.3	0.0	0.0
277.9	0.3	9.3	0.0	11.6	0.1	0.0	27.9	0.7	0.0	0.7	27.9	0.0	0.13	11.6	0.0	9.3	0.3
277.9	0.3	9.3	0.0	11.6	0.1	0.0	27.9	0.7	0.0	0.7	27.9	0.0	0.13	11.6	0.0	9.3	0.3
299.7	0.0	0.0	30.3	0.0	0.0	19.4	0.0	0.0	0.5	0.0	0.0	19.4	0.0	0.0	30.3	0.0	0.0
323.3	0.1	34.5	0.0	1.9	4.6	0.0	5.1	3.9	0.0	3.9	5.1	0.0	4.6	1.9	0.0	34.5	0.1
323.3	0.1	34.5	0.0	1.9	4.6	0.0	5.1	3.9	0.0	3.9	5.1	0.0	4.6	1.9	0.0	34.5	0.1
350.2	0.0	2.7	0.0	1.0	5.4	0.0	2.6	38.1	0.0	38.1	2.6	0.0	5.4	1.0	0.0	2.7	0.0
350.2	0.0	2.7	0.0	1.0	5.4	0.0	2.6	38.1	0.0	38.1	2.6	0.0	5.4	1.0	0.0	2.7	0.0
379.4	0.0	0.0	1.6	0.0	0.0	5.6	0.0	0.0	85.5	0.0	0.0	5.6	0.0	0.0	1.6	0.0	0.0

	Principal *g* values		
Energy (cm^{-1})	g_x	g_y	g_z
0.00	0.00	0.00	4.64
0.00	0.00	0.00	4.64
12.7	0.00	0.00	0.00
17.9	0.00	0.00	0.40
17.9	0.00	0.00	0.40
80.0	0.00	0.00	0.00
104.3	0.00	0.00	15.39
104.3	0.00	0.00	15.39
259.4	0.00	0.00	0.00
277.9	0.00	0.00	2.46
277.9	0.00	0.00	2.46
299.7	0.00	0.00	0.00
323.3	0.00	0.00	12.04
323.3	0.00	0.00	12.04
350.2	0.00	0.00	3.31
350.2	0.00	0.00	3.31
379.4	0.00	0.00	0.00

Tabble S14. Energies (cm^{-1}), percentage composition of the CASSCF/RASSI wavefunctions and the principal *g* values of **1-Er.**

	$\|m_J\rangle$															
Energy (cm^{-1})	**+15/2**	**+13/2**	**+11/2**	**+9/2**	**+7/2**	**+5/2**	**+3/2**	**+1/2**	**−1/2**	**−3/2**	**−5/2**	**−7/2**	**−9/2**	**−11/2**	**−13/2**	**−15/2**
0.0	0.0	0.5	0.7	0.0	3.3	4.4	0.0	25.0	55.3	0.0	2.0	7.4	0.0	0.3	1.1	0.0
0.0	0.0	1.1	0.3	0.0	7.4	2.0	0.0	55.3	25.0	0.0	4.4	3.3	0.0	0.7	0.5	0.0
45.3	0.0	39.5	2.4	0.0	4.6	2.0	0.0	1.4	1.4	0.0	2.0	4.6	0.0	2.4	39.5	0.0
45.3	0.0	39.5	2.4	0.0	4.6	2.0	0.0	1.4	1.4	0.0	2.0	4.6	0.0	2.4	39.5	0.0
54.3	0.6	0.0	0.0	18.8	0.0	0.0	33.0	0.0	0.0	41.6	0.0	0.0	6.1	0.0	0.0	0.0
54.3	0.0	0.0	0.0	6.1	0.0	0.0	41.6	0.0	0.0	33.0	0.0	0.0	18.8	0.0	0.0	0.6
90.3	0.0	10.4	1.6	0.0	0.0	0.9	0.0	0.6	0.0	0.0	29.9	0.0	0.0	56.3	0.3	0.0
90.3	0.0	0.3	56.3	0.0	0.0	29.9	0.0	0.0	0.6	0.0	0.9	0.0	0.0	1.6	10.4	0.0
278.5	0.0	0.0	0.0	0.2	0.0	0.0	2.2	0.0	0.0	6.7	0.0	0.0	16.6	0.0	0.0	74.4
278.5	74.4	0.0	0.0	16.6	0.0	0.0	6.7	0.0	0.0	2.2	0.0	0.0	0.2	0.0	0.0	0.0
331.5	0.0	2.6	5.5	0.0	12.0	6.4	0.0	11.1	2.3	0.0	30.8	2.5	0.0	26.4	0.5	0.0
331.5	0.0	0.5	26.4	0.0	2.5	30.8	0.0	2.3	11.1	0.0	6.4	12.0	0.0	5.5	2.6	0.0
399.5	0.0	3.2	1.9	0.0	37.2	9.4	0.0	1.6	1.2	0.0	12.3	28.4	0.0	2.4	2.4	0.0
399.5	0.0	2.4	2.4	0.0	28.4	12.3	0.0	1.2	1.6	0.0	9.4	37.2	0.0	1.9	3.2	0.0
399.6	24.0	0.0	0.0	54.0	0.0	0.0	15.7	0.0	0.0	0.9	0.0	0.0	4.4	0.0	0.0	1.1
399.6	1.1	0.0	0.0	4.4	0.0	0.0	0.9	0.0	0.0	15.7	0.0	0.0	54.0	0.0	0.0	24.0

	Principal *g* values		
Energy (cm^{-1})	g_x	g_y	g_z
0.0	9.17	9.17	1.62
45.3	3.56	3.56	12.2
54.3	0.00	0.00	4.72
90.3	2.94	2.94	7.77
278.5	0.00	0.00	15.24
331.5	6.63	6.63	4.56
399.5	7.41	6.90	4.52
399.6	0.15	0.25	11.10

Table S15. Energies (cm^{-1}), percentage composition of the CASSCF/RASSI wavefunctions and the principal *g* values of **1-Tm.**

	$\|m_J>$												
Energy (cm^{-1})	**6**	**5**	**4**	**3**	**2**	**1**	**0**	**−1**	**−2**	**−3**	**−4**	**−5**	**−6**
0.00	7.2	0.0	0.0	32.2	0.0	0.0	21.1	0.0	0.0	32.2	0.0	0.0	7.2
34.4	9.3	0.0	0.0	36.1	0.0	0.0	9.2	0.0	0.0	36.1	0.0	0.0	9.3
40.8	0.0	6.4	1.8	0.0	33.7	8.1	0.0	8.1	33.7	0.0	1.8	6.4	0.0
40.8	0.0	6.4	1.8	0.0	33.7	8.1	0.0	8.1	33.7	0.0	1.8	6.4	0.0
78.2	0.0	0.9	17.5	0.0	7.3	24.2	0.0	24.2	7.3	0.0	17.5	0.9	0.0
78.2	0.0	0.9	17.5	0.0	7.3	24.2	0.0	24.2	7.3	0.0	17.5	0.9	0.0
263.9	14.8	0.0	0.0	4.5	0.0	0.0	61.4	0.0	0.0	4.5	0.0	0.0	14.8
346.4	41.0	0.0	0.0	8.8	0.0	0.0	0.4	0.0	0.0	8.8	0.0	0.0	41.0
348.8	0.0	0.3	30.5	0.0	1.6	17.6	0.0	17.6	1.6	0.0	30.5	0.3	0.0
348.8	0.0	0.3	30.5	0.0	1.6	17.6	0.0	17.6	1.6	0.0	30.5	0.3	0.0
380.6	27.6	0.0	0.0	18.5	0.0	0.0	7.8	0.0	0.0	18.5	0.0	0.0	27.6
468.7	0.0	42.3	0.1	0.0	7.4	0.2	0.0	0.2	7.4	0.0	0.1	42.3	0.0
468.7	0.0	42.3	0.1	0.0	7.4	0.2	0.0	0.2	7.4	0.0	0.1	42.3	0.0

	Principal *g* values		
Energy (cm^{-1})	g_x	g_y	g_z
0.00	0.0	0.0	6.96
34.4	0.0	0.0	6.96
40.8	0.0	0.0	3.90
40.8	0.0	0.0	3.90
78.2	0.0	0.0	3.49
78.2	0.0	0.0	3.49
263.9	0.0	0.0	0.00
346.4	0.0	0.0	0.00
348.8	0.0	0.0	6.29
348.8	0.0	0.0	6.29
380.6	0.0	0.0	0.00
468.7	0.0	0.0	10.50
468.7	0.0	0.0	10.50

Table S16. Energies (cm^{-1}), percentage composition of the CASSCF/RASSI wavefunctions and the principal *g* values of **1-Yb.**

	$\|m_J>$							
Energy (cm^{-1})	7/2	5/2	3/2	1/2	−1/2	−3/2	−5/2	−7/2
0.00	15.7	0.0	0.0	61.4	0.0	0.0	22.9	0.0
288.9	0.0	0.0	93.0	0.0	0.0	7.0	0.0	0.0
304.6	3.2	53.6	0.0	3.9	9.4	0.0	22.1	7.8
526.3	1.5	1.4	0.0	0.5	24.8	0.0	0.0	71.8

	Principal *g* values		
Energy (cm^{-1})	g_x	g_y	g_z
0.00	3.94	0.66	3.94
288.9	3.41	0.00	0.00
304.6	3.29	1.11	1.11
526.3	6.07	1.73	1.73

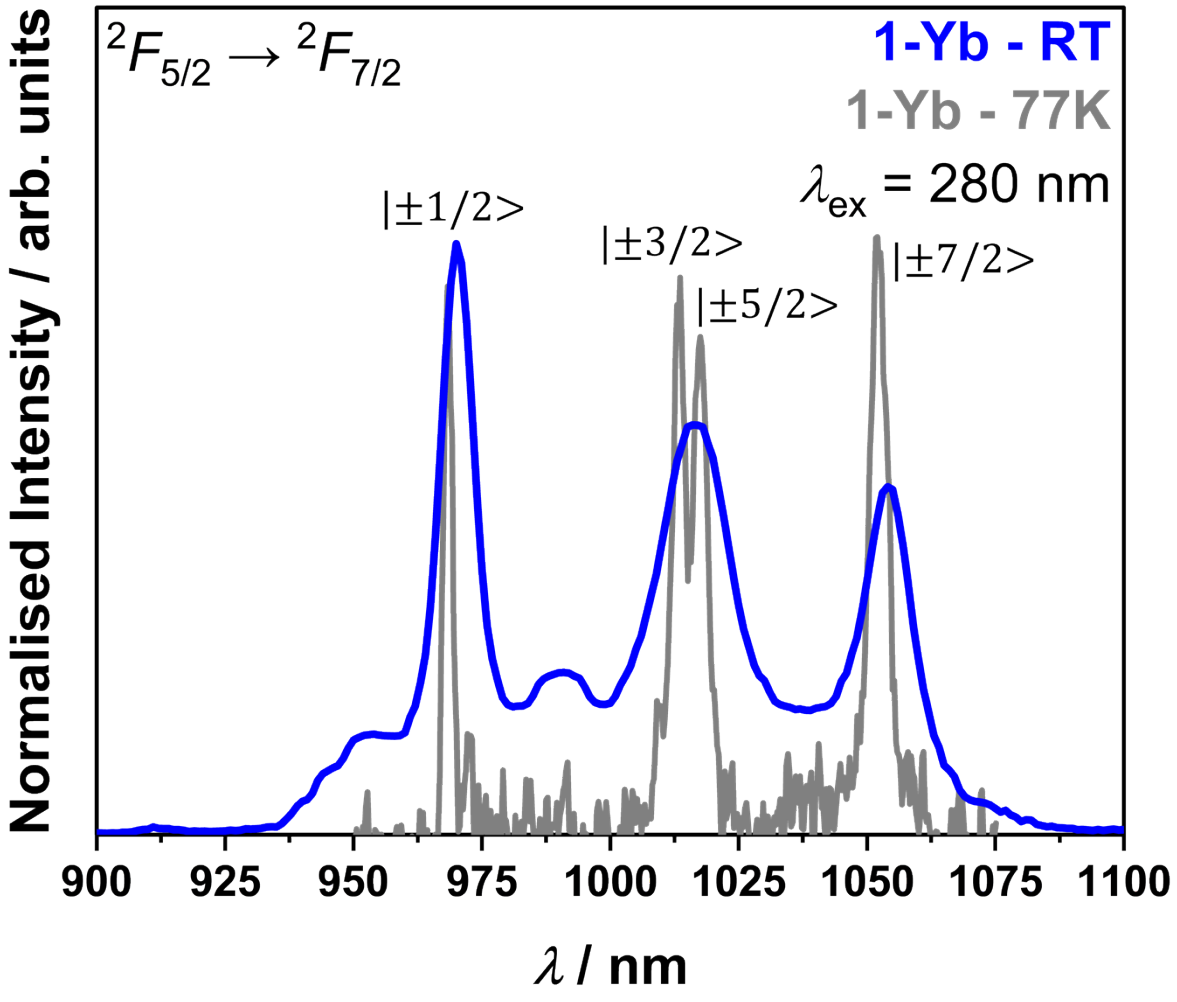

Figure S28. Emission spectra of compound **1-Yb**·0.5MeCN at room temperature (blue) and 77 K (grey). Excited at 280 nm.